New insights into sorption and desorption of organic phosphorus on goethite, gibbsite, kaolinite and montmorillonite

Issifou Amadou, Michel-Pierre Faucon, David Houben

1   **New insights into sorption and desorption of organic phosphorus on goethite,**

2   **gibbsite, kaolinite and montmorillonite**

3   Issifou Amadou[a*,] Michel-Pierre Faucon[a] and David Houben[a]

4   [a] AGHYLE (SFR Condorcet FR CNRS 3417), UniLaSalle, 19 Rue Pierre Waguet, 60026 Beauvais,

5   France

6   *corresponding author: Issifou.Amadou@unilasalle.fr

7   **Highlights**

8   • Mineral properties and organic P (OP) characteristics affected OP (de)sorption

9   • Myo-inositol hexakisphosphate had higher adsorption than the other OP forms

10   • Organic P showed contrasted adsorption capacities relative to inorganic P forms (IP)

11   • Fe and Al oxides exhibited highest adsorption capacity compared to clay minerals

12   • Organic P was more desorbed from clays minerals than from Fe and Al oxides

13   **Abstract**

14   With the increasing use of organic resource for P fertilization, the adsorption and desorption dynamics

15   of various organic phosphorus (OP) forms remain an important gap of knowledge to bridge in order to

16   improve P availability. In this study, we examined the adsorption and desorption dynamics of various

17   OP (myo-inositol hexakisphosphate, myo-IHP; glycerophosphate, GLY; and glucose-6-phosphate,

18   G6P) compounds to and from several soil minerals including Fe and Al oxides (goethite and gibbsite,

19   respectively) and clays minerals (kaolinite and montmorillonite). Overall, myo-IHP was the most

20   adsorbed form followed by G6P and then GLY which reflected that OP adsorption increased according

21   to the number of phosphate groups and/or the size of the organic molecule. Fe and Al oxides showed

22   higher OP adsorption capacity than clays, as adsorption followed the trend kaolinite < montmorillonite

23   < goethite <<<< gibbsite.

24   Desorption experiments revealed that the adsorption was not fully reversible as only 30% could

25   easily desorbed. On Fe and Al oxides, G6P and GLY were more desorbed than myo-IHP while the

26   opposite trend was found on clay minerals. In addition, OP desorption from soil minerals followed the

27   trend gibbsite < goethite < kaolinite < < montmorillonite. The clay-OP complex released P rapidly but

28   over a short period of time, whereas the Fe- and Al-OP complex released P slowly but over a longer

29   period of time. The comparison between the P adsorption and desorption properties of montmorillonite

30   and other soil minerals are only valid for the K-saturated montmorillonite used here. The results could

31   be different if the montmorillonite were saturated with Al or Ca. By deciphering the interactions between

32   soil minerals and the predominant forms of OP in soils and organic fertilizers, our results provide new

33   insights for the sustainable management of P in agroecosystems.

34   **Keywords:** Adsorption; desorption; organic phosphorus; phosphorus availability; soil fertility

35   **1. Introduction**

36   Phosphorus (P) is one of the essential nutrients required for plant growth and an important driver of

37   agroecosystem productivity (Hu et al., 2020a; Ruttenberg and Sulak, 2011). Due to its low solubility

38   and high affinity for mineral surfaces (Roy et al., 2017; Tisdale and Nelson, 1966), P availability is

39   limited in agricultural soils and rarely sufficient for optimum growth and development of crops. On the

40   other hand, accumulation of P in the soil increases the risk of P leaching and runoff, consequently leading

41   to eutrophication of surface waters (Hansen et al., 2002). Therefore, with the increasing use of organic

42   resources as P fertilizers(Amadou et al., 2021), a sustainable and efficient use of organic P (OP)

43   fertilizers is of utmost importance to secure future crop production and reduce environmental

44   hazard(Faucon et al., 2015). However, most of the research investigating the fate of P applied to the soil

45   has focused on inorganic P (IP) so far, showing that most of it was adsorbed onto iron (Fe) and aluminum

46   (Al)-oxides and clays minerals (Celi et al., 2000, 1999) or precipitated with Ca (Houben et al., 2011;

47   Urrutia et al., 2013). In contrast, the fate of OP has been disregarded so far even though it is now clear

48   that these forms of P can be at least as available as IP (Amadou et al., 2021; Kahiluoto et al., 2015).

49 Organic P can be mineralized along with plant uptake and/or be protected by organic substances from

50 adsorption, even in the long term (Huang and Zhang, 2012). However, the adsorption mechanisms of

51 OP and the factors that affect sorbing processes remain poorly understood (Yan et al., 2014) and there

52 is still a lack of knowledge about their contribution to plant nutrition (Faucon et al., 2015).

53   Organic P in soil-plant-system comes from both soil and organic waste sources (e.g. manure,

54 compost, sludge, biochar, …) (Fuentes et al., 2006). The major OP compounds from soil and organic

55 wastes include myo-IHP (Turner et al., 2002; Vincent et al., 2013), GLY (Doolette et al., 2011; Newman

56 and Tate, 1980) and G6P (Deiss et al., 2018; Giles et al., 2011). Each form differs from the others by its

57 P content, P bond type and molecular size. They may constitute large fractions of the total P in soils

58 (Monbet et al., 2009), especially in organic waste-amended soils (Khare et al., 2004). It has been shown

59 that adsorption of OP compounds increases with the number of P groups. Therefore, with six phosphate

60 groups, myo-IHP has a high charge density and would undergo a strong interaction with the soil

61 (Anderson and Arlidge, 1962; Celi et al., 1999). This higher accumulation of myo-IHP through

62 adsorption limits P acquisition by plants from this source. The size and molecular structure of OP forms

63 generally affect their adsorption capacity. The G6P adsorption density and rate is higher than myo-IHP

64 and adenosine triphosphate (ATP) as a result of its lower molar mass (Giaveno et al., 2008). However,

65 Goebel et al., (2017) reported that G6P is potentially more available than myo-IHP and ATP.

66   After adsorption, the ability of soil minerals to release P in soil solution determines P availability

67 for plants but also loss of P in both surface runoff and subsurface flow (Sharpley et al., 2001). Several

68 authors have suggested that P from mineral-P complexes is not available to plants because of their very

69 limited desorption (Barrow, 1986; Bollyn et al., 2017; Guzman et al., 1994; Lagos et al., 2016). For

70 instance, Bollyn et al., (2017) showed that after several cycles of desorption, less than 5% P desorbed

71 from myo-IHP-goethite complexes. Similar results by Lagos et al., (2016) showed limited desorption of

72 myo-IHP (<3% P) from gibbsite. On the other hand, there is also experimental evidence that P can

73 desorb significantly from minerals to be available to plants and runoff (Andrino et al., 2019; Parfitt,

74 1979). However, in all of these studies cited above, the form of P used was exclusively IP with very

75 limited consideration for important OP pools such as IHP, GLY or G6P. Furthermore, the soil minerals

76 used were in most cases Fe oxides (namely goethite) while Al oxides and clay minerals were much less

investigated. To our knowledge, no study has evaluated and compared P desorption from the main OP compounds (IHP, GLY, and G6P) that were adsorbed onto the main soil minerals (Fe and Al oxides, and clay minerals). There is a need to bridge this gap of knowledge to identify the properties that govern OP adsorption and desorption processes and gaining insight into the behavior of OP compounds at the surface of soil minerals.

In sum, extensive research has evaluated the adsorption of different individual sources of organic and inorganic P to soils or to individual soil minerals. However, no study has evaluated and compared P desorption from the main OP compounds that were adsorbed onto the main soil minerals. The aim of our study was to elucidate the dynamics of adsorption and desorption of several forms of OP on several representative soil minerals. More specifically, we aimed at determining the drivers of adsorption and desorption of OP on soil minerals. For this purpose, we studied the adsorption of three OP compounds, myo-inositol hexakisphosphate (myo-IHP), glycerophosphate (GLY) and glucose-6-phosphate (G6P) and one inorganic compound (KH_2PO_4, IP) on Fe and Al oxides (goethite and gibbsite, respectively) and on clay minerals (kaolinite and montmorillonite). Organic P sources were chosen based on their predominance in both soils and organic inputs and their contrasted chemical properties. We assume that the selected Fe, Al oxides and clay minerals, abundant in the soils, will present different capacities of adsorption and desorption due to their chemical properties.

2. Materials and methods

2.1. Organic P forms and individual soil minerals

Three organic P (OP) compounds, myo-IHP, GLY, G6P and one IP (KH_2PO_4) (Fig.1) were selected based on their predominance in organic wastes and soils and their contrasted properties (type of P bonds, different molecular sizes). The individual soil minerals were selected to be representative of the predominant soil minerals involved in P adsorption in soils. Four individual soil minerals were used. Goethite [FeO(OH)] and gibbsite [Al (OH)$_3$] were chosen as representative of Fe and Al oxides; kaolinite and montmorillonite were selected as clay minerals, particularly 1:1 phyllosilicate and 2:1 phyllosilicate respectively. The minerals used have different specific surface areas (SSA) and points of

4

103 zero charge (PZC). The SSA of the minerals used are as follows: goethite (46 m^2 g^{-1}), gibbsite (120-364

104 m^2 g^{-1}), kaolinite (19 m^2 g^{-1}) and K-montmorillonite (83 m^2 g^{-1}) and their PZCs were: goethite (7.04),

105 gibbsite (9.3), kaolinite (4.5) and montmorillonite (2.5), as previously reported by other authors (He et

106 al., 1994; He and Zhu, 1997; Ruttenberg and Sulak, 2011; Shang et al., 1990; Yan et al., 2014). All

107 minerals were obtained from Sigma-Aldrich Chemie S.a.r.l. and VWR (France) for experimentation (see

108 supplementary data references in supplementary data (Table S1) for mineral references)
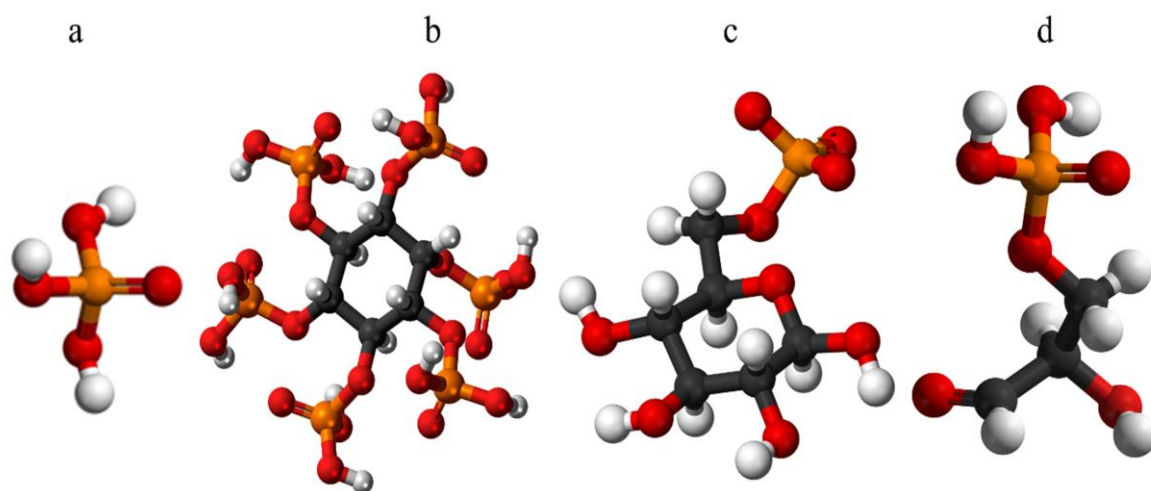
109

110 Fig.1. Chemical structure of potassium dihydrogen phosphate, IP (a), myo-inositol hexakisphosphate,

111 IHP (b), β-D-Glucopyranose-6-phosphate, G6P (c) and Glycerol phosphate, GLY(d).

112 2.2. Adsorption Experiments

113 Triplicate batch experiments were conducted to understand the interactions between OP forms and soils

114 minerals at different P concentrations. We used standard P adsorption procedure proposed by Nair et

115 al., (1984). Prior to adsorption, 80mg of each soil mineral were weighed and transferred to 50 mL

116 polypropylene centrifuge tubes. Then, 20 ml of 0.1 M KCl were added and the tubes were shaken for 24

117 hours at 25°C to sufficiently hydrate the adsorption sites on the minerals. The pH was maintained at 5.5

118 ± 0.05 by adding 0.1 M HCl or NaOH solution. Six P concentrations (0, 4, 8, 16, 40, 75 and 100 mg L^{-1}

119) were used for each P forms. Phosphorus stock solutions of each OP were prepared under the same

120 conditions of 0.1 M KCl at pH 5.5. KCl was used as electrolyte to mimic the environmental condition

5

121   and adjust ionic strength of the solution. To start the adsorption, 20 ml of solution containing each

122   concentration of P were pipetted into tubes containing the soil particles. The control experiment was the

123   same but without P. The final volume was 40 mL and the concentration of particles in this final volume

124   was 2 g L^{-1}. In each tube, some drops of hexanol were added to suppress microbial activities. The final

125   samples were shaken on a mechanical shaker for 24 hours at 25°C and then centrifuged (3000 g for 15

126   minutes). After centrifugation, samples were immediately filtered through a 0.22-μm membrane syringe

127   filter. The filtrates were stored in a cold room until the P content was analyzed. Inorganic P was

128   determined colorometrically (Ohno and Zibilske, 1991). Organic P compound samples was hydrolyzed

129   to IP form before colorimetric determination by using the persulfate oxidation method (Peters and Van

130   Slyke, 1932). The quantity of P adsorbed was calculated as the difference between the initial amount of

131   P added and the remaining P amount in solution at the end of the adsorption experiment. Adsorption

132   maxima, capacity and other adsorption parameters were determined by fitting data to the non-linear

133   form of the Langmuir (1) and Freundlich (2) isothermal model (Crini et al., 2007; Langmuir, 1918):

134    $Q_{ads} = Qm\, K_L\, [Ce/\, (1+ K_L\, Ce)]$ (1) ;

135   where Ce is the concentration of P in the equilibrium solution (mg L^{-1}), Q_{ads} is the total amount of P

136   adsorbed, K_L is the affinity constant or binding energy (L mg^{-1}), and Qm is the P adsorption maxima

137   (μg g^{-1}). The ability of soil minerals to resist a change in solution P concentration was measured as the

138   maximum adsorption buffer capacity: MBC = $K_L \times (Qm)$; where K_L and Qm are the binding-energy

139   related constant and maximum adsorption, respectively, in the Langmuir equation.

140    $Q_{ads} = K_F\, Ce^{1/nF}$ (2);

141   where Q_{ads} (μg g^{-1}) is the total amount of P adsorbed, Ce is the adsorbate equilibrium concentration in

142   solution, K_F (μmol L^{-1}) is adsorption capacity, and nF (mmol L^{-1}) is Freundlich exponent.

143   2.3. Desorption kinetics experiments

144   Prior to desorption, the four soil minerals were loaded with the three OP compounds or IP. Solutions

145   containing 1 g P L^{-1} in 0.1 M KCl at pH 5.5 were prepared using the different P compounds. Goethite,

146   gibbsite, kaolinite and montmorillonite was weighed in portions of 100 g into 1L bottles containing.

6

147   Then, 200 ml of 0.1 *M* KCl were added and the bottles were shaken for 24 hours at 25°C to sufficiently

148   hydrate the adsorption sites on the minerals. The pH was maintained at 5.5 ± 0.05 by adding 0.1 *M* HCl

149   or NaOH solution. To start the complex formations, each of the 1L bottles containing the soil minerals

150   was filled with 800 ml of P solutions. This was done in order to obtain all the mineral-P complexes, for

151   example for goethite we will have: goethite-IP, goethite-IHP, goethite-G6P and goethite-GLY and

152   similarly for the other minerals. In each 1L bottles containing both the soil minerals and P compounds,

153   some drops of hexanol were added to suppress microbial activities. The final samples containing in the

154   bottles were shaken on a mechanical shaker for 24 hours at 25°C and then centrifuged (3000 g for 15

155   minutes). The 1L bottles were distributed into several small 250-mL bottles, centrifuged, and the

156   supernatants were collected. Centrifugation was repeated until the maximum volume of supernatants

157   was removed. The produced P-loaded minerals was agitated in deionized water and frozen at -20∘C. The

158   amounts of adsorbed P were determined using the same procedure as described in Section 2.2. The

159   amounts of adsorbed P (μgP g^{-1}) were similar to the Qm values (Table 1) of the adsorption data

160   (Section 2.2) that were predicted by the Langmuir model.

161   Desorption kinetics experiments were initiated by adding 40 ml of 0.1 *M* KCl adjusted to pH

162   5.5 to 0.5g of the different minerals-P complex. Samples were shaken on a mechanical shaker at 25°C

163   at regular intervals (24h, 48h, 72h, 96h). After the first cycle (24h), the entire suspension was removed

164   and immediately filtered through a 0.22-μm membrane filter. A fresh 40 ml solution of 0.1 *M* KCl was

165   added to start the second cycle (48h). The same process was applied for the remaining cycles. The P

166   concentration in the supernatant was determined as described above. Desorption maxima and rate were

167   determined by fitting data to the non-linear form of the Elovich kinetic model (Bulut et al., 2008) (3):

168      $Q = A + B * Lnt$ (3);

169   where q is the amount of P desorbed at time t, and A and B are the constants with $A = \frac{1}{\beta}$ and $B =$

170      $\frac{1}{\beta} Ln\alpha\,\beta$ (α and β are the constants in the original formula of Elovich equation). The A value (mgP kg^{-1})

171   in the Elovich equation is the amount of P desorbed in the first day of desorption (q = A +B*ln t, A = q

172   when t = 1) and that B (mgP day^{-1}) is positively related with the P desorption rate as demonstrated in

7

173   the studies of (He and al. 1994). A and B values have been used to compare P release rate in different

174   soils (He and Zhu, 1997). The maximum desorption amount (Dm) was calculated as total amount P

175   desorbed.

176   2.4. Statistical analysis

177   All the Langmuir, Freundlich and Elovich model's parameters were evaluated by non-linear regression

178   method using function *nls* from *Package 'nlstools'* in R software. Nonlinear parameter estimates can be

179   obtained using different methods (Archontoulis and Miguez, 2015; Bates and Watts, 1988); the most

180   common is ordinary least squares, which minimizes the sum of squared error between observations and

181   predictions (Brown, 2001). The determination coefficient (R^2) for each parameter was used to measure

182   the goodness-of-fit. Apart from R^2, standard errors (S.E.) were also used to determine the best-fitting

183   isotherm to the experimental data. The conceptual framework was performed using *correlate* and

184   *network plot* function in the latest development version of the *corr package* (Ahmed et al., 2021). This

185   generates a network graph of a correlation data frame in which variables that are more highly correlated

186   appear closer together and are connected by stronger paths. The proximity of points is determined using

187   multidimensional clustering.

188   **3. Results**

189   3.1. Dynamics of Organic Phosphorus Adsorption

190   3.1.1. Effect of OP forms on adsorption dynamics

191   Organic P adsorption differed for each specific OP compounds (Table 1). The strongest differences in

192   OP adsorbed among the different isotherms occurred with the greatest initial OP concentrations (Fig.

193   2). In addition, the magnitude of OP adsorption increased rapidly when the initial OP concentration was

194   low (< 25 mg L^{-1}), but became relatively slow with increasing concentration (up to 40 mg L^{-1}). Each OP

195   compound had different adsorption characteristics onto the various soil minerals. The Qm, i.e. maximum

196   OP adsorption capacity from the Langmuir equation (Table 1) ranged from 1045 µg g^{-1} to 56697µg g^{-1},

197   indicating marked variations in the amount of OP adsorbed. Among the OP compounds, myo-IHP was

198   the most adsorbed form (3742-56697 µg g^{-1}) followed by G6P and then GLY (1045-6237 µg g^{-1}) (Fig.

199   2 and Table 1). The adsorption maxima of OP increased with increasing molar mass in this order: GLY

200   (172 g mol^{-1}) < G6P (260 g mol^{-1}) < myo-IHP (660 g mol^{-1}), which showed that the size of the molecule

201   would have favored the adsorption of OP compounds.

202   Compared to IP, a contrasted adsorption behavior of OP compounds was observed. The

203   adsorption dynamics followed the trend myo-IHP > IP > G6P > GLY, showing that myo-IHP was more

204   adsorbed than IP, which in turn was more adsorbed than the G6P and GLY forms (Fig. 2 and Table 1).

205   The K_L value, i.e. the binding energy between OP and minerals surfaces were highly variable. With the

206   exception of montmorillonite, GLY or G6P showed higher or equal binding strength compared myo-

207   IHP (Table 1). Our results showed that the adsorption dynamics of OP was strongly controlled by their

208   biogeochemical properties in the soil. The myo-IHP, GLY and G6P form showed a different adsorption

209   process from each other as well as from the IP form. In general, myo-IHP was found to be the most

210   adsorbed P form and GLY the least adsorbed form.
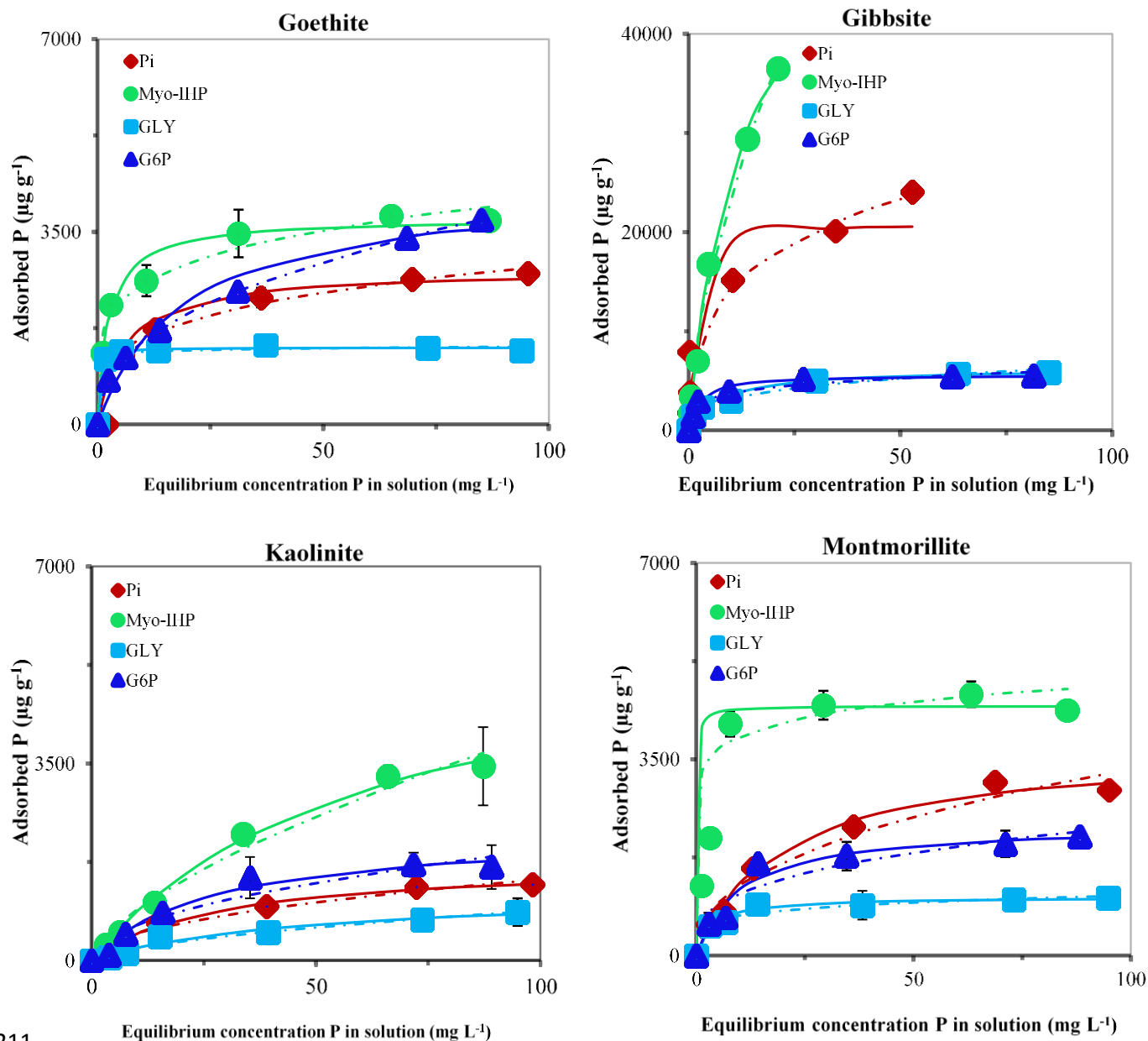
Fig. 2. Adsorption isotherms of OP forms by different soil minerals in 0.1 *M* KCl at pH 5.5: Symbols are data points, solid lines are Langmuir isotherms, and dashed lines are Freundlich isotherms. Gibbsite was different from other minerals because of the large difference in the maximum adsorption amount. Values of adsorbed quantities (Qads) and error bars (Se) are also provided as supplementary data (Table S2).

Table 1. Isotherm parameters of the Langmuir and Freundlich models for P adsorption.

Soil components	P Forms	Langmuir equation				Freundlich equation		
		Q_m (µg g^{-1})	K_L (L mg^{-1})	R^2	MBC (L Kg^{-1})	K_F	n	R^2
Goethite	IP	2810	0.16	0.97	450	848	3.77	0.99
	myo-IHP	3742	0.4	0.97	1497	1584	4.88	0.98
	GLY	1398	3.31	0.99	4626	1228	9.7	0.99
	G6P	4337	0.05	0.98	217	561	2.35	0.99
Gibbsite	IP	20949	0.99	0.91	20740	7158	3.31	0.96
	myo-IHP	56698	0.08	0.99	4536	5703	1.62	0.99
	GLY	6237	0.14	0.97	873	1584	3.26	0.98
	G6P	5588	0.4	0.98	2235	2254	4.58	0.96
Kaolinite	IP	1736	0.04	0.99	69	157	2.08	0.98
	myo-IHP	6082	0.02	0.99	122	197	1.53	0.98
	GLY	1222	0.02	0.96	24	57	1.68	0.96
	G6P	2295	0.04	0.98	92	198	2.01	0.92
Montmorillonite	IP	3709	0.05	0.99	185	465	2.34	0.97
	myo-IHP	4857	0.32	0.97	1554	1966	4.82	0.87
	GLY	1045	0.28	0.98	293	477	5.71	0.96
	G6P	2338	0.1	0.96	234	521	3.1	0.92

Q_m: maximum adsorption capacity, K_L: binding-energy related constant, R^2: model fitting degree, MBC: maximum buffer capacity (ability of soil minerals to resist a change in solution P concentration).

219

220

221   3.1.2. Adsorption dynamics as affected by soil minerals

222   Isotherms of OP adsorption for the four tested minerals demonstrated that OP adsorption patterns of the

223   Fe and Al oxides (goethite and gibbsite, respectively) were very similar but quite different from that of

224   clays minerals (montmorillonite and kaolinite) (Fig. 1). Fe and Al oxides rapidly adsorbed OP and their

225   adsorption maximum was reached at a lower initial concentration than for clays. All tested minerals

226   fitted the Langmuir and Freundlich equation (Table 1). Adsorption capacity (K_F) of OP by soil minerals

227   followed the trend kaolinite < montmorillonite < goethite << Gibbsite (Table 1), showing a marked

228   variability between the adsorption capacities of the tested soil minerals. The Fe and especially Al oxides

229 exhibited the highest maximum adsorption capacity for all OP forms. The specific surface area (SSA)

230 of soil minerals may differently affect their ability to sorb OP compounds. Our result showed that the

231 larger the SSA of soil minerals, the greater their ability to sorb IP forms. However, this was not

232 consistent for the OP compounds. For instance, kaolinite showed greater myo-IHP adsorption than

233 goethite and montmorillonite despite its smaller specific surface area.

234   The K_L value, i.e. the binding-energy-related constant obtained from the Langmuir equation

235 varied in the following order clays $\ll$ Fe and Al oxides (Table 1). The highest binding energy for

236 adsorbed OP was observed with goethite and the lowest with kaolinite. In addition, the maximum

237 buffering capacity of adsorption (MBC) of the Fe and Al oxides was much larger than for the clay

238 mineral (Table 1). Compared to IP, goethite and montmorillonite are more strongly bonded to OP;

239 however, the opposite was found on gibbsite and kaolinite, which bond IP more strongly than OP.

240 Therefore, despite the highest OP adsorption capacity of gibbsite, its interaction with OP would be less

241 strong than with IP. The results for the adsorption capacity and binding energy of montmorillonite are

242 only valid for the K-saturated montmorillonite used in this study. Al or Ca saturated montmorillonite

243 would result in different adsorption mechanisms. Fig. 6 illustrates a conceptual framework showing the

244 relationship between soil mineral properties (PZC, SSA) and Langmuir model adsorption parameters

245 (K_L and Qm). A positive relationship was found between the ability of soil minerals to adsorb and

246 strongly bind OP and the chemical and physical properties of the soil minerals (PZC, SSA).

247 3.2. Dynamics of Organic Phosphorus Desorption

248 3.2.1. Role of OP compounds in desorption dynamics.

249 In general, OP desorption by KCl was well fitted with Elovich equation, with determination coefficient

250 from 0.91 to 0.99 (Table 2). In this study, KCl was found to desorb a variable portion of adsorbed OP

251 from the tested OP-mineral complexes. The portion of OP desorbed from all soil minerals was lower

252 than the initially adsorbed OP (Fig. 3 and Table 2) which indicates that the adsorption was not fully

253 reversible, as a large amount remained adsorbed. Overall, P desorption was high on the first day (up to

254 30%) and then slowed down from the second to the fourth day (Fig. 3 and Table 2).

255   The Dm values refer to the predicted maximum desorption capacity of OP obtained from the

256   Elovich model (Table 2). Organic P compounds showed different Dm trends by mineral type. Both G6P

257   and GLY showed higher Dm values (13%-56%) than myo-IHP (3%-14.44%) on Fe and Al oxides. On

258   clay minerals, the pattern was rather opposite, with myo-IHP desorption being higher than other OP

259   forms (Table 2). The desorption maxima of all of the OP compounds were 4%-56%, lower than those

260   of IP which were between 13 % to 70% (Table 2 and Fig. 3), showing a general lower desorption of OP

261   relative to IP. However, there were some exceptions with G6P and/or GLY which showed higher

262   desorption than IP on Fe and Al oxides. The amount of OP desorbed could be related to the strength

263   with which it was bound to soil minerals (adsorption parameter K_L). The Fig. 6 showed negative

264   correlations between Dm and K_L, indicating that the amount of OP desorbed tends to decrease with

265   increasing OP binding energy to the soil minerals.

266   The rate of OP desorbed per day (A) predicted by the Elovich model varied widely for each OP-

267   mineral complex (Table 2). Most of OP-minerals complexes showed lower desorption rates per day than

268   IP-minerals. In addition, the different OP-mineral complexes can be classified according to desorption

269   rates into three categories (Fig. 4): low desorption rate complexes (<5% per day) which include all the

270   OP desorbed from gibbsite and kaolinite; medium desorption rate complexes (10-20% per day)

271   including myo-IHP and G6P from montmorillonite and high desorption rate complexes (20% > per day)

272   which include only G6P from goethite (Fig. 3).
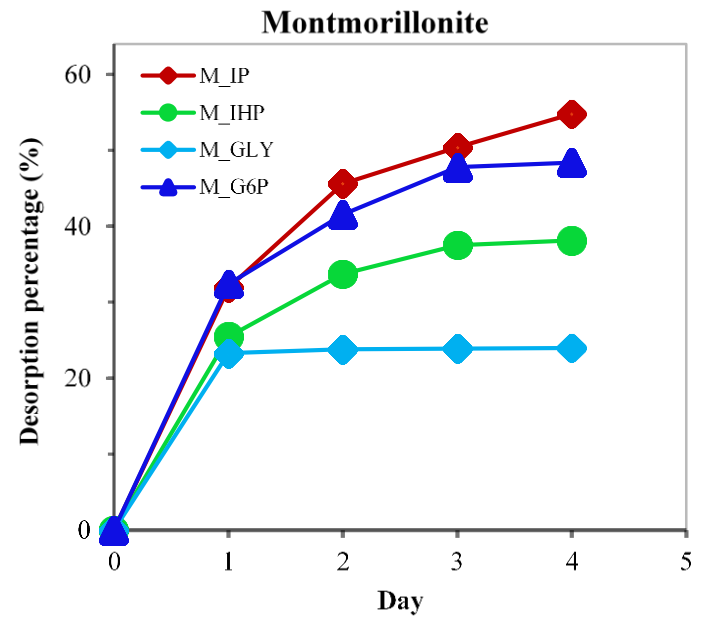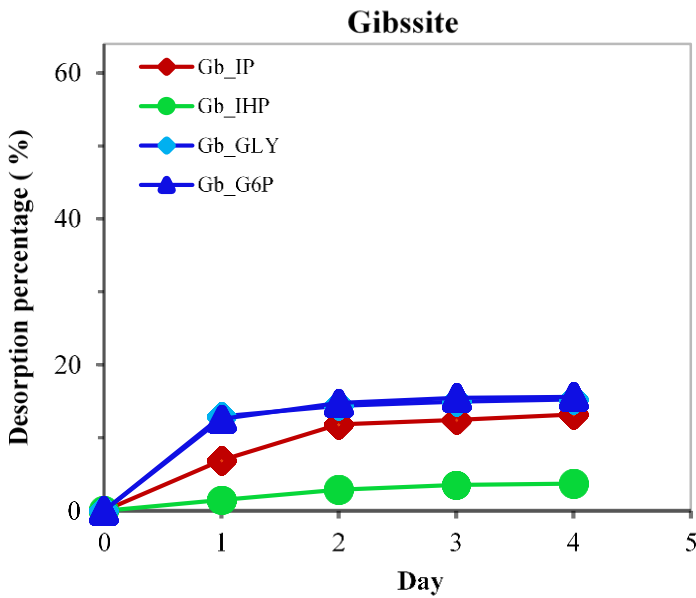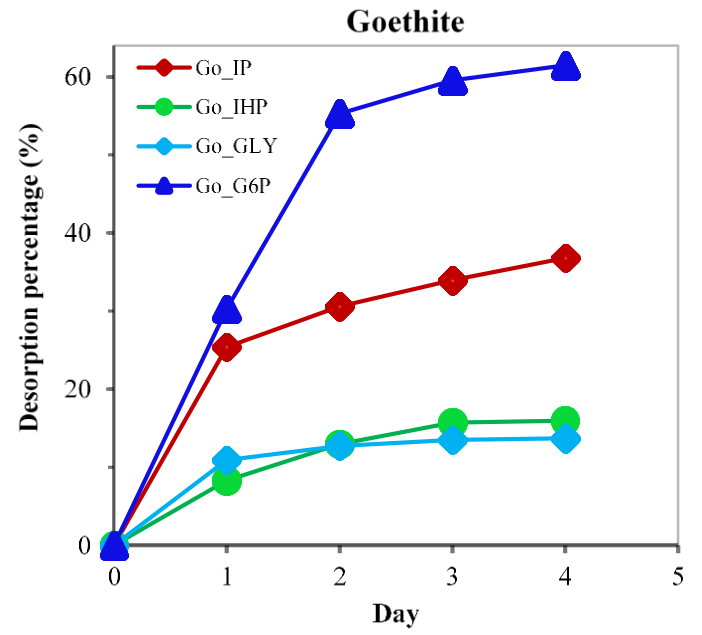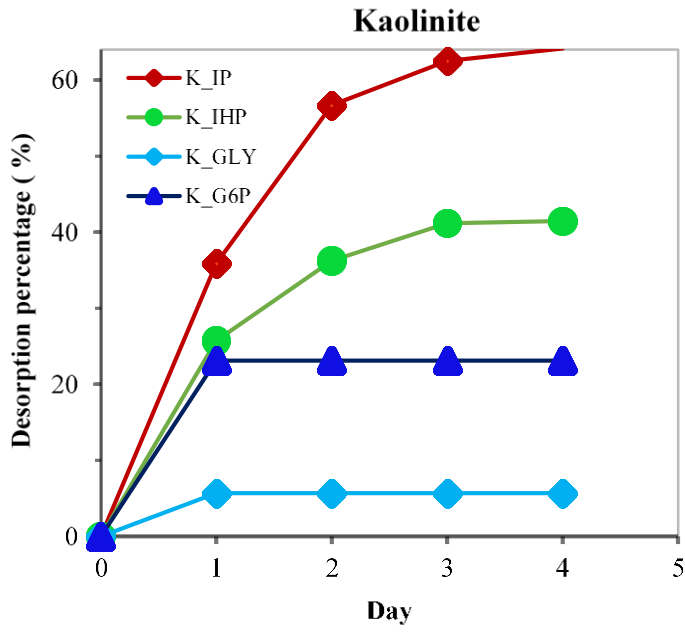
273

274

275   Fig. 3. Desorption kinetics of myo-IHP, GLY and G6P by 0.1 M KCl at pH 5.5 and at 25°C.

276   Table 2. Organic P desorption isotherm parameters of the Elovich model.

Soil components	P Forms	Elovich equation			
		Dm (%P g^{-1})	A (%P day^{-1})	B (%P g^{-1})	R^2
Goethite	IP	33	8	25	0.99
	myo-IHP	14	6	9	0.97
	GLY	13	2	11	0.97
	G6P	56	23	33	0.90
Gibbsite	IP	12	5	7	0.91
	myo-IHP	3	2	2	0.97
	GLY	15	2	13	0.98
	G6P	15	2	13	0.94
Kaolinite	IP	59	21	38	0.94
	myo-IHP	39	12	27	0.95
	GLY	6	0.01	6	0.98
	G6P	23	0.01	23	0.98
Montmorillonite	IP	49	16	33	0.99
	myo-IHP	36	10	26	0.96
	GLY	24	0	23	0.92
	G6P	45	12	33	0.97

Dm: maximum P desorption capacity, A: P desorption rate, B: amount of P desorbed in the first day of desorption in this study ($q = A + B * Lnt$, $B = q$ when $t = 1$), R^2: model fitting degree.

277

278
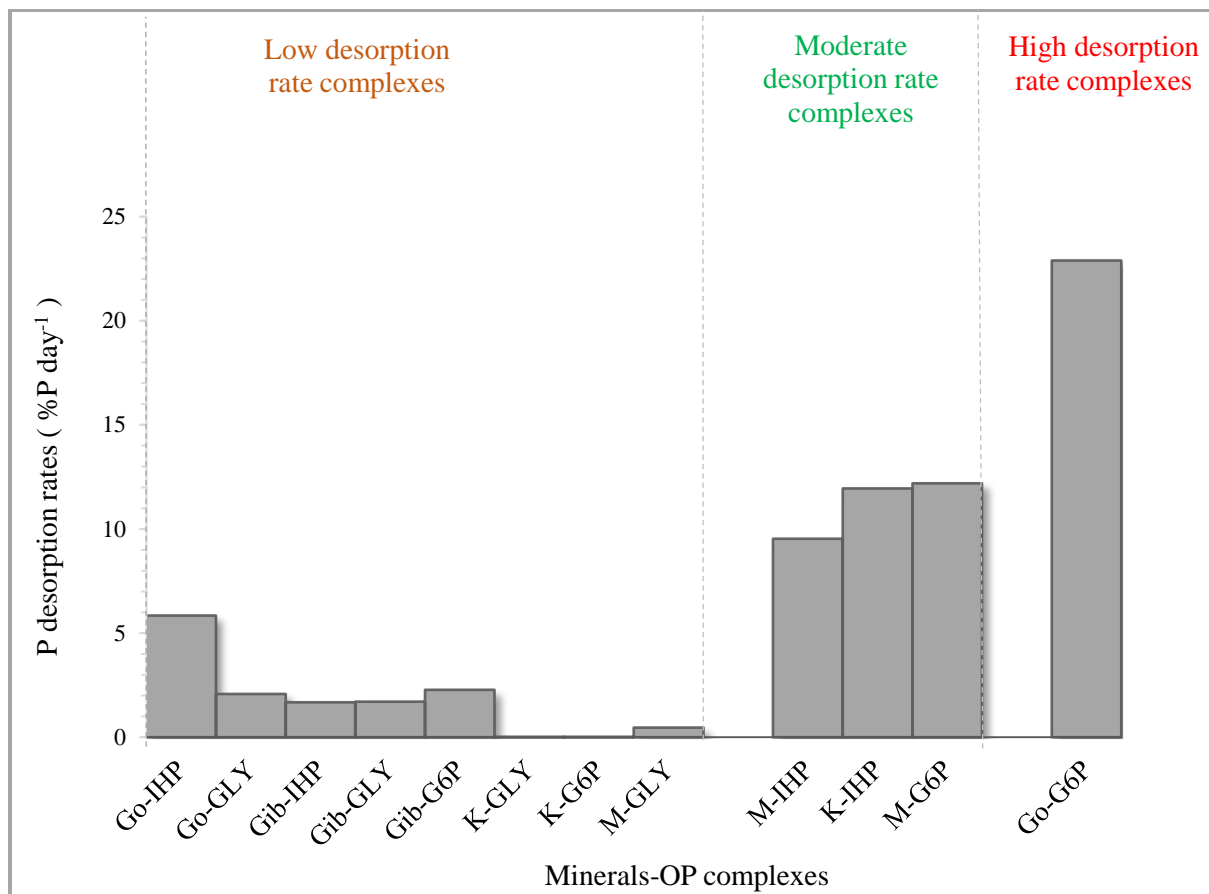
Fig. 4. Variation in P desorption rates of mineral-OP complexes.

3.2.2. Role of soil minerals in desorption dynamics

There was a large difference between Fe and Al oxides minerals and clays mineral with respect to desorption properties (Table 2 and Fig. 3). Phosphate desorption from Fe and Al oxides was very rapid, and equilibrium was attained within 2 days. Except for G6P on goethite, OP desorption from soil minerals at the end of the experiment could be ranked as gibbsite (3-14%) < goethite (13-14%) < kaolinite (5-39%) << montmorillonite (23-45%) (Table 2, Fig. 3). Organic P desorption from clays minerals was thus much higher than from Fe and especially Al oxides. This large difference in the capacity of soil minerals to release OP would be related to the physicochemical properties of the soil and the OP. Indeed, our results showed strong negative correlation between the desorption capacity (Dm) and the properties of the soil minerals (PZC and SSA), and the correlation appears to be stronger with PZC (Fig. 6).

292   Successive desorption (Fig. 5) using KCl showed that more than 25% of the adsorbed OP (myo-

293   IHP, G6P, GLY) on montmorillonite was desorbed in the first cycle and there was no desorption after 4

294   cycles. Compared to the clays-myo-IHP complex, P desorbed from Fe, A1 oxide- myo-IHP was lower

295   but declined more slowly with increasing number of cycles (Fig. 5). The same trends were observed

296   with the Fe andA1 oxide-GLY complexes. For instance, at the first cycle, more myo-IHP and GLY was

297   desorbed from the clay minerals than from the Fe and A1 oxides, but from the second cycle, Fe and Al

298   oxides had desorbed almost as much myo-IHP and GLY as the clays. At the fourth cycle, the amount of

299   myo-IHP and GLY desorbed from the clay minerals was lower or equal to that from Fe and A1 oxides.

300   This suggests that the clays-myo-IHP and GLY complex supplied P rapidly but over a short period

301   whereas the Fe and A1 oxide-IHP and GLY complex supplied P slowly but over a long period. With

302   slight differences, the soil mineral-G6P complexes appeared to show the same trend as mineral-IHP or

303   GLY. As mentioned above for the results of the adsorption mechanisms of montmorillonite, the

304   desorption properties (kinetics, amount and rate of desorption) are also only valid for K-saturated

305   montmorillonite.

306
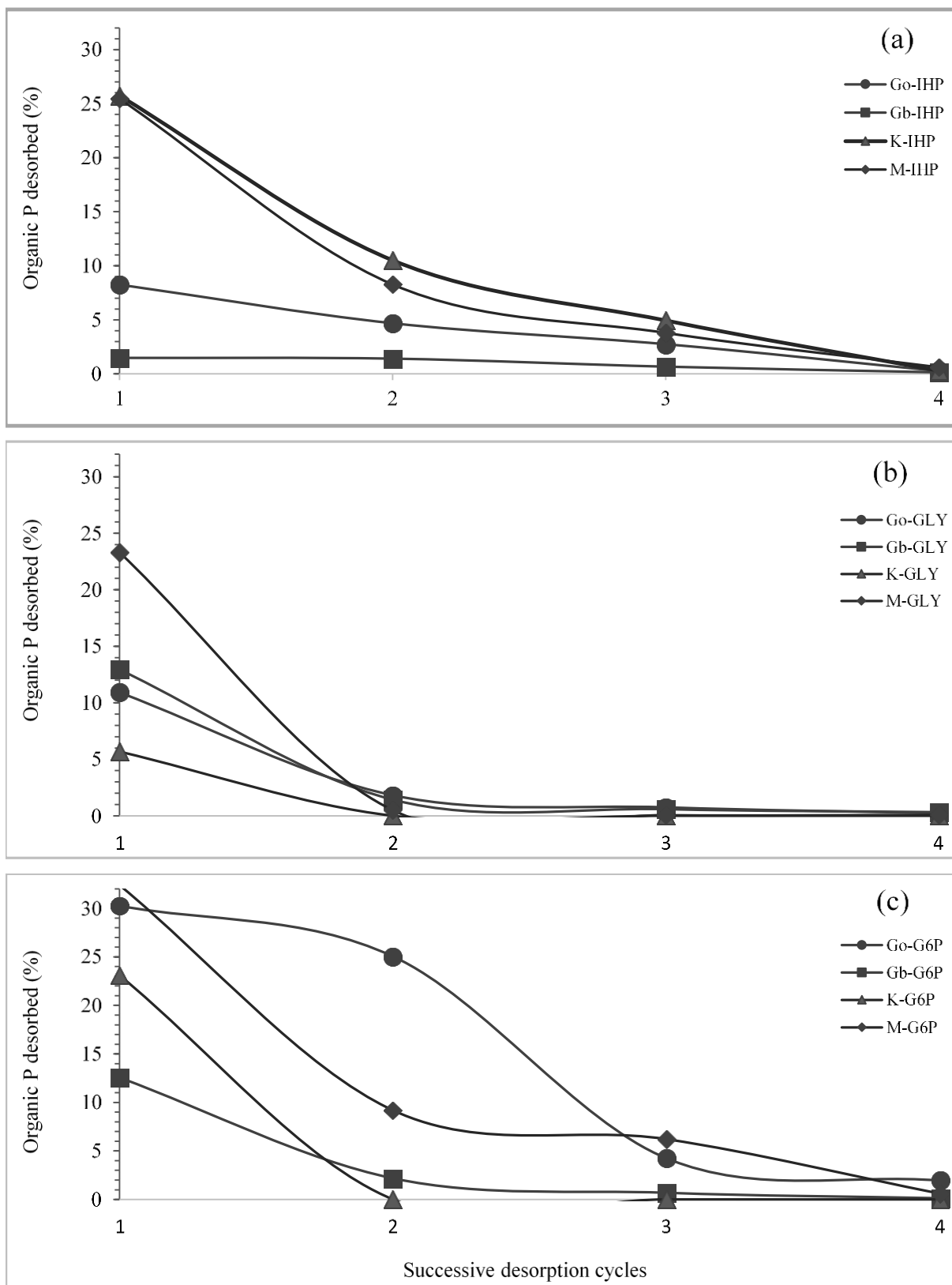
Fig. 5. Successive desorption of (a) IHP, (b) GLY and (c) G6P from OP-mineral complexes by KCl.

307
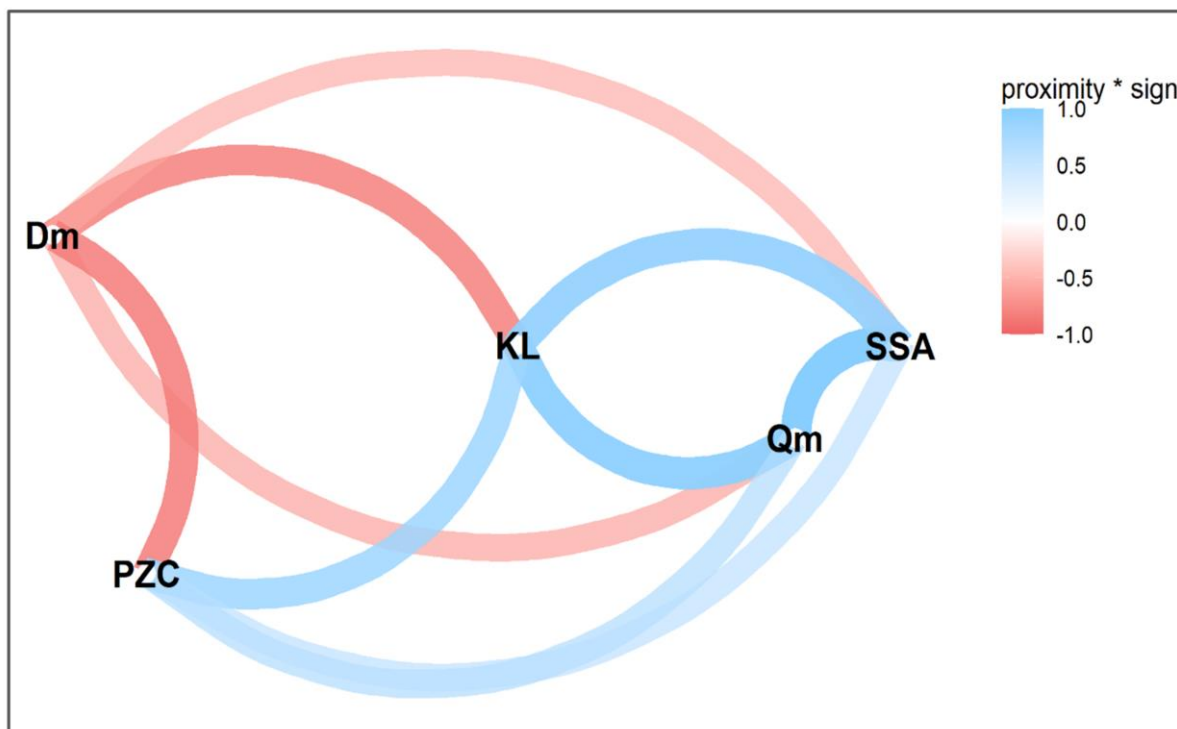
308

309 Fig. 6. Conceptual framework showing the linkage among soil minerals properties (PZC, SSA) and

310 adsorption/desorption parameters (bonding strength, K_L; adsorption capacity, Qm, and desorption

311 capacity, Dm). *The linkage is based on the relationships between different variables. The color of each*

312 *line refers to the degree of relationship between the variables. $R^2 > 0.5$*

4. Discussion

313

314 4.1. Influence of organic phosphorus properties on adsorption and desorption dynamics

315 Adsorption dynamics of OP compounds play an important role in the potential reactivity of OP in soils

316 amended with organic input. Our results showed the positive relationship between OP adsorption

317 dynamics and the number of phosphate groups of the organic molecule. The higher phosphate group

318 number, the higher the adsorption. Thus, myo-IHP, which has six orthophosphates per C moiety, was

319 adsorbed in larger quantities than the orthophosphate monoesters (G6P and GLY) because it can

320 coordinate with more hydroxyl (OH) groups on the surface of soil minerals (McKercher and Anderson,

321 1968). The sizes of the C moiety, may be also responsible for the difference in adsorption amount of

322 each OP compounds. Our results about molecular mass effects on OP adsorption dynamics were in

19

323 disagreement with most studies that found decreases in OP adsorption with increasing molecular mass

324 due to steric hindrance effects (Lü et al., 2017; Ruttenberg and Sulak, 2011). They specifically disagree

325 with those of Lü et al., (2017) who observed that the adsorption maxima of OPs on goethite and hematite

326 were classified as follows: IP > Adenosine monophosphate (AMP) = G6P > ATP, showing a decreasing

327 trend in sorption levels with increasing molecular mass of the different forms of OP. Our results also

328 contrast with those of Yan et al., (2014) where the maximum sorption densities of three Al

329 (oxyhydr)oxides (amorphous $Al(OH)_3$, boehmite and α-Al_2O_3) increased with decreasing molecular

330 massas follows IHP < ATP < G6P < GLY < IP. However, the results obtained agree with the work of

331 Berg and Joern, (2006), which showed a trend of increasing rather than decreasing sorption levels with

332 increasing molecular mass of different forms of OP (IHP > G6P > ATP > IP). Similarly, recent work by

333 Ganta et al., (2020) and Ahmed et al., (2021) also supported our results. They demonstrated that the

334 organic fraction of the OP may not influence the interaction of individual phosphate groups with the soil

335 and thus the effect of molecular mass steric hindrance may be insignificant.

336   After adsorption, the ability of OP compounds to desorb depends not only on their chemical

337 properties but also on the degree of energy with which they are adsorbed onto soil minerals (Ganta et

338 al., 2021, 2019). A general weaker or equal binding strength of myo-IHP compared to GLY or G6P was

339 found. This disagrees with recent results that reported total interaction energies (in absolute value)

340 measured for goethite-IHP complexes (-72 to -85 kcal mol^{-1}) higher than those for GLY (-38 to -48 kcal

341 mol^{-1}) (Ganta et al., 2019; Kubicki et al., 2012; Rakovan et al., 1999). In addition, this finding also

342 contradicts the extensive literature that associates the large amount of IHP adsorbed with its strong

343 binding to minerals (Celi et al., 2000; Giaveno et al., 2008; Guan et al., 2006; Johnson et al., 2012; Xu

344 et al., 2017). However, this indicates that the higher adsorption of IHP relative to other OP compounds

345 did not necessarily imply that its binding capacity is always strong and stable under all environmental

346 conditions. Thus, we suggest that despite the higher accumulation of myo-IHP reported in most soils

347 (Amadou et al., 2021; Gerke, 2015), its desorption may be easier than that of the GLY or G6P forms,

348 although this depends greatly on the soil minerals and experimental conditions . Furthermore, our results

349 indicated that if both GLY and G6P species compete with myo-IHP for the same active sites on soil

350 minerals, the binding energy of GLY or G6P would be higher than that of myo-IHP. Therefore, one

351　could expect easier desorption of myo-IHP from soil compared to GLY and G6P even though this would

352　be highly dependent on soil minerals.

353　4.2. Influence of soil mineral characteristics on adsorption and desorption dynamics

354　The tested soil minerals presented a different capacity to sorb OP compounds due to their contrasting

355　physicochemical properties. Fe and Al oxides showed very different OP adsorption mechanisms

356　compared to clays, as the adsorption capacity ranked as follows: kaolinite < montmorillonite < goethite

357　<<< gibbsite. This can be explained by their contrasting types of surface charge. At pH 5.5 (pH used for

358　this study), kaolinite has a small net negative charge, goethite has a small net positive charge and gibbsite

359　is positively charged while montmorillonite is negatively charged according to their PZC values (He et

360　al., 1994; He and Zhu, 1997). Gibbsite exhibited the greatest adsorption maximum, which was probably

361　related to the combined effect of its high surface positive charge and greater SSA (120-364 m^2 g^{-1}), as

362　well as the abundance of active adsorption sites, as noted by Shang et al., (1990) and Yan et al., (2014).

363　Manning and Goldberg, (1996) found that gibbsite and goethite adsorbed roughly 23 times more P than

364　kaolinite and up to 53.5 times more IP than montmorillonite and illite. However, despite the highest OP

365　adsorption capacity of gibbsite, its interaction energy with OP would be less strong than IP. The order

366　of the K_L value, i.e., binding energy (clays << Fe and Al oxides), suggests a much higher binding energy

367　between OP and Fe and Al oxides than between OP and clays. These results suggest that the mechanism

368　of OP adsorption on Fe and Al oxides is quite different from that on clay minerals. In sum, soil minerals

369　had diverse adsorption mechanisms, specifically Fe and Al oxides compared to clay minerals. The

370　changes in their adsorption and binding capacity to OP compounds were the result of their contrasting

371　physicochemical properties. This may result in different behavior in the desorption of adsorbed Po.

372　However, since it is well known that the number of positive charges of variably charged minerals

373　(especially Fe and Al oxyhydroxides and kaolinite) decreases with increasing pH, we speculate that their

374　adsorption may decrease at higher pH than that of our study (i.e. pH> 5.5)(Hu et al., 2020b). In addition,

375　it is also known that cations in solution can affect the P sorption potential of certain minerals, e.g., Al

376　or Ca saturated clay minerals (Ellis Jr and Truog, 1955; Pissarides et al., 1968; Prietzel et al., 2016). The

377 next challenge will be therefore to elucidate the role various cations on OP retention by minerals. This

378 could also allow to feed surface complexation models to gain in robustness on the understanding of the

379 adsorption and desorption mechanisms while better predicting P behavior in soils.

380   The desorption dynamics of the adsorbed OP was markedly affected by both OP and soil

381 minerals characteristics. OP was more desorbed from clays minerals (montmorillonite and kaolinite)

382 than from Fe and Al oxides. Since clays have also been shown to have a lower OP retention capacity, it

383 can be expected that OP will be more available when organic inputs are applied to soils dominated by

384 phyllosilicates, e.g. subtropical and temperate soils (Bortoluzzi et al., 2015; He et al., 1994).

385 Furthermore, with time, OP desorption kinetics and rate differed between soil minerals. Our findings

386 showed that clays-OP complex released P rapidly but over a short period whereas the Fe and A1 oxide-

387 OP complex released slowly but over a longer period. In the clay-OP complexes, the binding energy

388 would be unstable and its distribution would have varied remarkably with time, probably from loosely-

389 bound fraction to tightly-bound fraction. In contrasts, Fe and Al oxide-OP complexes were stable with

390 time. These results indicated that each complex would have presented a different binding mechanism,

391 e.g. the inner sphere versus the outer sphere complex with different types of bonds e.g. bidentate versus

392 monodentate (Ganta et al., 2019). Our results highlighted the central role of OPs and their interactions

393 with soil minerals on P availability and potential P loss to water. Better knowledge of these interactions

394 constitutes an important challenge to model OP dynamics and predict P release to plants and waters in

395 soil amended with OP fertilizers. Despite the overall low desorption of OP from Fe and Al complexes,

396 G6P and GLY were however more desorbed from goethite and gibbsite than IP. This weaker retention

397 of these OP forms by Fe and Al oxides suggests that both G6P and GLY could be used in Fe/Al oxide-

398 rich soils to improve P nutrition of plants. This has therefore great implication for P fertilization in

399 highly weathered soils of tropical regions in which Fe and/or Al oxides are dominant. Taken together,

400 our results indicate that both Fe and Al oxides and clay minerals in soil could be either OP sinks or OP

401 sources, depending on their properties, binding energy and adsorption saturation.

402   It must be noted, however, that soils may contain a much wider variety of Fe and Al oxides

403 than those used in this study, namely goethite and gibbsite respectively. For example, many soils contain

404 significant amounts of ferrihydrite, which was reported to have a higher P sorption than goethite

405   (Prietzel et al., 2016; Ruttenberg and Sulak, 2011; Prietzel and Klysubun, 2018). As an outlook, we

406   strongly suggest studies to better understand the involvement of a wide range of iron oxides in the

407   dynamics of OP forms. More generally, though our results provide a mechanistic understanding of the

408   sorption processes of various OP forms on selected soil minerals, the role of other soil minerals alone

409   or in combination needs still to be investigated to generate a better overview of OP dynamics in real

410   complex soil systems. In addition, it is also important to point out that our results regarding the

411   comparison between the P (de)sorption properties of montmorillonite and other soil minerals are only

412   valid for the K-saturated montmorillonite used here. For Al- or Ca-saturated montmorillonite, a much

413   stronger P sorption or less pronounced P desorption would be expected compared to K-saturated

414   montmorillonite. Furthermore, in agroecosystems, with the exception of periods immediately following

415   heavy K fertilization, K-saturated montmorillonite, which was used here as the montmorillonite type, is

416   rare in most soils. Thus, the results must be considered in light of the type of clay used (K-saturated

417   montmorillonite in this study).

418   4.3. Adsorption and desorption dynamics of OP relative to IP

419   Compared to IP, myo-IHP was generally more strongly adsorbed whereas the opposite was observed

420   for G6P and GLY. This result showed that specific forms of OP, depending on their characteristics, had

421   contrasting adsorption dynamics with respect to IP. Therefore, the weaker retention of OP compared to

422   IP which is generally suggested in the literature (Anderson et al., 1974; Condron et al., 2015, 2005) did

423   not apply to all organic P compounds as higher inositol phosphate esters can be strongly retained in soil.

424   Berg and Joern, (2006) found that soils pretreated with myo-IHP or having combinations of myo-IHP

425   and IP in solution had reduced IP adsorption by successfully competing for binding sites, indicating that

426   there was a preference in the adsorption of myo-IHP over IP. This preference may either lead to the

427   release of already adsorbed IP or prevent further adsorption of IP, leading to an increase in both available

428   IP for plants and soluble IP for runoff (Leytem et al., 2002). Furthermore, in the presence of different

429   OP forms in soils, the preferential adsorption of myo-IHP or IP over both G6P and GLY may increase

430   G6P and GLY availability and promote their mineralization. Thus, this contrasting adsorption dynamics

431   of OP versus IP have important implications for P management from organic input in soils because IHP,

432   GLY and G6P can comprise up to 80% of total P in some organic input (Amadou et al., 2021; Darch et

433   al., 2014; George et al., 2018), and many animal manures, notably those from monogastrics (pigs,

434   poultry), contain substantial quantities of inositol phosphates (Hu et al., 2020a; Peperzak et al., 1959).

435   Application of these manures to agricultural land could, therefore, promote the solubilization of IP

436   and/or reduce the adsorption of G6P and GLY which would then be available for uptake by plants but

437   also released into runoff water (Reid et al., 2018). On most soil minerals, the amount of desorbed OP

438   and the desorbed rate of OP were generally lower than those of IP. After several desorption cycles, (Roy

439   et al., 2017) found that 20% of IP desorbed from goethite while it only accounted for less than 5% for

440   OP. Similar findings were reported by (Ruyter-Hooley et al., 2016) with limited desorption of OP (<3%

441   of total amount) on gibbsite, even in the presence of humic acids as competing ligands for sorption sites.

442   Huang and Zhang, (2012) showed that OP compounds added by organic input may desorb slowly and

443   mineralized in step with plant uptake, even in the long term. However, our results showed that this did

444   not apply to all OP compounds.

5. Concluding remarks

446   Moving toward more sustainable sources for managing P nutrition in agroecosystems, OP derived from

447   organic inputs and soil is increasingly considered to complement mineral P fertilizer. However,

448   enhancing OP cycling and availability in soils while reducing OP loss into the environment requires a

449   better understanding of OP adsorption/desorption processes on soil minerals. Factors related to soil

450   properties and OP molecular characteristics directly affect the reactions of OP and its release into the

451   soil. The myo-IHP, GLY and G6P form showed different adsorption processes from each other as well

452   as from the IP form. Our results demonstrated contrasted adsorption capacities between myo-IHP and

453   the other organic P forms (G6P and GLY) relative to IP form, with myo-IHP exhibiting the greatest

454   adsorption capacities. The adsorption capacity of each OP compounds is determined by the number of

455   orthophosphate groups associated with the C moiety in each compound and its size. The general idea of

456   a lower adsorption of OP relative to IP suggested by the literature does not match for all OP compounds

457   since, even though myo-IHP was more strongly retained relative to IP, G6P and GLY were more weakly

458   retained. In general, OP compounds showed less desorption and slower desorption rate per day than IP

459   forms. Fe and Al oxides showed very different OP adsorption mechanisms compared to clays regarding

460   their binding energy and adsorption amount, which were related to different in properties (SSA and

461   PZC). The Fe and especially Al oxides (gibbsite) exhibited the highest maximum adsorption capacity

462   for all OP forms.

463   The desorption dynamics of the adsorbed OP was markedly affected by both OP and soil

464   minerals characteristics. Montmorillonite showed the highest desorption for OP suggesting higher OP

465   release when organic inputs are applied soils dominated by 2:1 phyllosilicate. However, the results are

466   very dependent on the specific type of montmorillonite used in this study. In fact, the results related to

467   the comparison between the P (de)sorption properties of montmorillonite and other soil minerals are

468   only valid for the K-saturated montmorillonite used here. If Al- or Ca-saturated montmorillonite, which

469   are the most common types of montmorillonite in soils, had been used, much higher P sorption and

470   lower P desorption would be expected compared to K-saturated montmorillonite. Finally, despite their

471   overall high adsorption, the higher desorption of G6P or GLY relative to IP from Fe and Al oxides

472   indicated that G6P and GLY release would be less affected than IP by such soil compounds, which are

473   especially abundant in highly weathered soils. However, since the P concentration used in our study

474   may be higher than that of real soil systems, it would be interesting to investigate the effect of P

475   concentration on adsorption processes by performing sorption experiments at different (and lower) P

476   concentrations.

477   By simultaneously analyzing the interactions between various OP forms and various soil

478   minerals, this study provides new insight into the OP adsorption and desorption dynamics on soil

479   minerals which is important to optimize the use of organic input as fertilizer and to improve or develop

480   prediction model of OP release in agroecosystems.

481   **Declaration of Competing Interest**

482   The authors declare that they have no known competing financial interests or personal relationships that

483   could have appeared to influence the work reported in this paper.

References

492 Ahmed, W., Jing, H., Kailou, L., Ali, S., Tianfu, H., Geng, S., Jin, C., Qaswar, M., Jiangxue,
493   D., Mahmood, S., Maitlo, A.A., Khan, Z.H., Zhang, H., Chen, D.-Y., 2021. Impacts of
494   long-term inorganic and organic fertilization on phosphorus adsorption and desorption
495   characteristics in red paddies in southern China. PLOS ONE 16, e0246428.
496   https://doi.org/10.1371/journal.pone.0246428

497 Amadou, I., Houben, D., Faucon, M.-P., 2021. Unravelling the Role of Rhizosphere
498   Microbiome and Root Traits in Organic Phosphorus Mobilization for Sustainable
499   Phosphorus Fertilization. A Review. Agronomy 11, 2267.
500   https://doi.org/10.3390/agronomy11112267

501 Anderson, G., Arlidge, E.Z., 1962. The adsorption of inositol phosphates and glycerophosphate
502   by soil clays, clay minerals, and hydrated sesquioxides in acid media. Journal of Soil
503   Science 13, 216–224. https://doi.org/10.1111/j.1365-2389.1962.tb00699.x

504 Anderson, G., Williams, E.G., Moir, J.O., 1974. A Comparison of the Sorption of Inorganic
505   Orthophosphate and Inositol Hexaphosphate by Six Acid Soils. Journal of Soil Science
506   25, 51–62. https://doi.org/10.1111/j.1365-2389.1974.tb01102.x

507 Andrino, A., Boy, J., Mikutta, R., Sauheitl, L., Guggenberger, G., 2019. Carbon Investment
508   Required for the Mobilization of Inorganic and Organic Phosphorus Bound to Goethite
509   by an Arbuscular Mycorrhiza (Solanum lycopersicum x Rhizophagus irregularis).
510   Frontiers in Environmental Science 7 (2019), Nr. 26 7. https://doi.org/10.15488/4844

511 Archontoulis, S.V., Miguez, F.E., 2015. Nonlinear Regression Models and Applications in
512   Agricultural Research. Agronomy Journal 107, 786–798.
513   https://doi.org/10.2134/agronj2012.0506

514 Barrow, N.J., 1986. Reaction of Anions and Cations with Variable-Charge Soils, in: Advances
515   in Agronomy. Elsevier, pp. 183–230. https://doi.org/10.1016/S0065-2113(08)60676-8

516 Bates, D., Watts, D.G., 1988. Nonlinear Regression Analysis and Its Applications.
517   https://doi.org/10.2307/1268866

518 Berg, A.S., Joern, B.C., 2006. Sorption Dynamics of Organic and Inorganic Phosphorus
519   Compounds in Soil. J. Environ. Qual. 35, 1855–1862.
520   https://doi.org/10.2134/jeq2005.0420

521 Bollyn, J., Faes, J., Fritzsche, A., Smolders, E., 2017. Colloidal-Bound Polyphosphates and
522   Organic Phosphates Are Bioavailable: A Nutrient Solution Study. J. Agric. Food Chem.
523   65, 6762–6770. https://doi.org/10.1021/acs.jafc.7b01483

524 Bortoluzzi, E.C., Pérez, C.A.S., Ardisson, J.D., Tiecher, T., Caner, L., 2015. Occurrence of iron
525   and aluminum sesquioxides and their implications for the P sorption in subtropical soils.
526   Applied Clay Science 104, 196–204. https://doi.org/10.1016/j.clay.2014.11.032

527 Brown, A.M., 2001. A step-by-step guide to non-linear regression analysis of experimental data
528   using a Microsoft Excel spreadsheet. Computer Methods and Programs in Biomedicine
529   65, 191–200. https://doi.org/10.1016/S0169-2607(00)00124-3

530 Bulut, E., Özacar, M., Şengil, İ.A., 2008. Adsorption of malachite green onto bentonite:
531   equilibrium and kinetic studies and process design. Microporous and mesoporous
532   materials 115, 234–246.

533 Celi, L., Lamacchia, S., Barberis, E., 2000. Interaction of inositol phosphate with calcite.
534   Nutrient Cycling in Agroecosystems 57, 271–277.
535   https://doi.org/10.1023/A:1009805501082

536 Celi, L., Lamacchia, S., Marsan, F.A., Barberis, E., 1999. Interaction of inositol hexaphosphate
537   on clays: adsorption and charging phenomena: soil science 164, 574–585.
538   https://doi.org/10.1097/00010694-199908000-00005

539 Condron, L.M., Turner, B.L., Cade-Menun, B.J., 2015. Chemistry and Dynamics of Soil
540   Organic Phosphorus, in: Thomas Sims, J., Sharpley, A.N. (Eds.), Agronomy
541   Monographs. American Society of Agronomy, Crop Science Society of America, and
542   Soil Science Society of America, Madison, WI, USA, pp. 87–121.
543   https://doi.org/10.2134/agronmonogr46.c4

544 Condron, L.M., Turner, B.L., Cade-Menun, B.J., 2005. Chemistry and Dynamics of Soil
545   Organic Phosphorus, in: Phosphorus: Agriculture and the Environment. John Wiley &
546   Sons, Ltd, pp. 87–121. https://doi.org/10.2134/agronmonogr46.c4

547 Crini, G., Peindy, H.N., Gimbert, F., Robert, C., 2007. Removal of C.I. Basic Green 4
548   (Malachite Green) from aqueous solutions by adsorption using cyclodextrin-based
549   adsorbent: Kinetic and equilibrium studies. Separation and Purification Technology 53,
550   97–110. https://doi.org/10.1016/j.seppur.2006.06.018

551 Darch, T., Blackwell, M.S.A., Hawkins, J.M.B., Haygarth, P.M., Chadwick, D., 2014. A Meta-
552   Analysis of Organic and Inorganic Phosphorus in Organic Fertilizers, Soils, and Water:
553   Implications for Water Quality. Critical Reviews in Environmental Science and
554   Technology 44, 2172–2202. https://doi.org/10.1080/10643389.2013.790752

555 Deiss, L., de Moraes, A., Maire, V., 2018. Environmental drivers of soil phosphorus
556   composition in natural ecosystems. Biogeosciences 15, 4575–4592.
557   https://doi.org/10.5194/bg-15-4575-2018

558 Doolette, A.L., Smernik, R.J., Dougherty, W.J., 2011. A quantitative assessment of phosphorus
559   forms in some Australian soils. Soil Research 49, 152–165.

560 Ellis Jr, R., Truog, E., 1955. Phosphate fixation by montmorillonite. Soil Science Society of
561   America Journal 19, 451–454.

562 Faucon, M.-P., Houben, D., Reynoird, J.-P., Mercadal-Dulaurent, A.-M., Armand, R., Lambers,
563   H., 2015. Advances and Perspectives to Improve the Phosphorus Availability in
564   Cropping Systems for Agroecological Phosphorus Management, in: Advances in
565   Agronomy. Elsevier, pp. 51–79. https://doi.org/10.1016/bs.agron.2015.06.003

566 Fuentes, B., Bolan, N., Naidu, R., Mora, M. de la L., 2006. Phosphorus in organic waste-soil
567   systems. R.C. Suelo Nutr. Veg. 6. https://doi.org/10.4067/S0718-27912006000200006

568 Ganta, P.B., Kühn, O., Ahmed, A.A., 2020. QM/MM molecular dynamics investigation of the
569   binding of organic phosphates to the 100 diaspore surface.

570 Ganta, P.B., Kühn, O., Ahmed, A.A., 2019. QM/MM simulations of organic phosphorus
571   adsorption at the diaspore–water interface. Phys. Chem. Chem. Phys. 21, 24316–24325.
572   https://doi.org/10.1039/C9CP04032C

573 Ganta, P.B., Morshedizad, M., Kühn, O., Leinweber, P., Ahmed, A.A., 2021. The Binding of
574   Phosphorus Species at Goethite: A Joint Experimental and Theoretical Study (preprint).
575   CHEMISTRY. https://doi.org/10.20944/preprints202102.0171.v1

576 George, T.S., Giles, C.D., Menezes-Blackburn, D., Condron, L.M., Gama-Rodrigues, A.C.,
577   Jaisi, D., Lang, F., Neal, A.L., Stutter, M.I., Almeida, D.S., Bol, R., Cabugao, K.G.,
578   Celi, L., Cotner, J.B., Feng, G., Goll, D.S., Hallama, M., Krueger, J., Plassard, C.,
579   Rosling, A., Darch, T., Fraser, T., Giesler, R., Richardson, A.E., Tamburini, F., Shand,
580   C.A., Lumsdon, D.G., Zhang, H., Blackwell, M.S.A., Wearing, C., Mezeli, M.M.,
581   Almås, Å.R., Audette, Y., Bertrand, I., Beyhaut, E., Boitt, G., Bradshaw, N., Brearley,
582   C.A., Bruulsema, T.W., Ciais, P., Cozzolino, V., Duran, P.C., Mora, M.L., de Menezes,
583   A.B., Dodd, R.J., Dunfield, K., Engl, C., Frazão, J.J., Garland, G., González Jiménez,
584   J.L., Graca, J., Granger, S.J., Harrison, A.F., Heuck, C., Hou, E.Q., Johnes, P.J., Kaiser,
585   K., Kjær, H.A., Klumpp, E., Lamb, A.L., Macintosh, K.A., Mackay, E.B., McGrath, J.,
586   McIntyre, C., McLaren, T., Mészáros, E., Missong, A., Mooshammer, M., Negrón, C.P.,
587   Nelson, L.A., Pfahler, V., Poblete-Grant, P., Randall, M., Seguel, A., Seth, K., Smith,
588   A.C., Smits, M.M., Sobarzo, J.A., Spohn, M., Tawaraya, K., Tibbett, M., Voroney, P.,
589   Wallander, H., Wang, L., Wasaki, J., Haygarth, P.M., 2018. Organic phosphorus in the
590   terrestrial environment: a perspective on the state of the art and future priorities. Plant
591   Soil 427, 191–208. https://doi.org/10.1007/s11104-017-3391-x

592 Gerke, J., 2015. Phytate (Inositol Hexakisphosphate) in Soil and Phosphate Acquisition from
593   Inositol Phosphates by Higher Plants. A Review. Plants 4, 253–266.
594   https://doi.org/10.3390/plants4020253

595 Giaveno, C., Celi, L., Cessa, R.M.A., Prati, M., Bonifacio, E., Barberis, E., 2008. Interaction
596   of organic phosphorus with clays extracted from oxisols. Soil Science 173, 694–706.
597   https://doi.org/10.1097/SS.0b013e3181893b59

598 Giles, C., Cade-Menun, B., Hill, J., 2011. The inositol phosphates in soils and manures:
599   Abundance, cycling, and measurement. Can. J. Soil. Sci. 91, 397–416.
600   https://doi.org/10.4141/cjss09090

601 Goebel, M.-O., Adams, F., Boy, J., Guggenberger, G., Mikutta, R., 2017. Mobilization of
602   glucose-6-phosphate from ferrihydrite by ligand-promoted dissolution is higher than of
603   orthophosphate.   J.   Plant   Nutr.   Soil   Sci.   180,   279–282.
604   https://doi.org/10.1002/jpln.201600479

605 Guan, X.-H., Shang, C., Zhu, J., Chen, G.-H., 2006. ATR-FTIR investigation on the
606   complexation of myo-inositol hexaphosphate with aluminum hydroxide. Journal of
607   Colloid and Interface Science 293, 296–302. https://doi.org/10.1016/j.jcis.2005.06.070

608 Guzman, G., Alcantara, E., Barron, V., Torrent, J., 1994. Phytoavailability of phosphate
609   adsorbed on ferrihydrite, hematite, and goethite. Plant Soil 159, 219–225.
610   https://doi.org/10.1007/BF00009284

611 Hansen, N.C., Daniel, T.C., Sharpley, A.N., Lemunyon, J.L., 2002. The fate and transport of
612   phosphorus in agricultural systems. Journal of Soil and Water Conservation 57, 408–
613   417.

614 He, Z.L., Yang, X., Yuan, K.N., Zhu, Z.X., 1994. Desorption and plant-availability of
615   phosphate   sorbed   by   some   important   minerals.   Plant   Soil   162,   89–97.
616   https://doi.org/10.1007/BF01416093

617 He, Z.L., Zhu, J., 1997. Transformation and bioavailability of specifically sorbed phosphate on
618   variable-charge minerals in soils. Biology and Fertility of Soils 25, 175–181.
619   https://doi.org/10.1007/s003740050300

620 Houben, D., Meunier, C., Pereira, B., Sonnet, Ph., 2011. Predicting the degree of phosphorus
621   saturation using the ammonium acetate-EDTA soil test: Degree of phosphorus
622   saturation in soils. Soil Use and Management no-no. https://doi.org/10.1111/j.1475-
623   2743.2011.00353.x

624 Hu, Z., Jaisi, D.P., Yan, Y., Chen, H., Wang, X., Wan, B., Liu, F., Tan, W., Huang, Q., Feng,
625   X., 2020a. Adsorption and precipitation of *myo* -inositol hexakisphosphate onto
626   kaolinite. Eur J Soil Sci 71, 226–235. https://doi.org/10.1111/ejss.12849

627 Hu, Z., Jaisi, D.P., Yan, Y., Chen, H., Wang, X., Wan, B., Liu, F., Tan, W., Huang, Q., Feng,
628   X., 2020b. Adsorption and precipitation of myo-inositol hexakisphosphate onto
629   kaolinite. European Journal of Soil Science 71, 226–235.

630 Huang, X.-L., Zhang, J.-Z., 2012. Hydrolysis of glucose-6-phosphate in aged, acid-forced
631   hydrolysed nanomolar inorganic iron solutions—an inorganic biocatalyst? RSC Adv. 2,
632   199–208. https://doi.org/10.1039/C1RA00353D

633 Johnson, B.B., Quill, E., Angove, M.J., 2012. An investigation of the mode of sorption of
634   inositol hexaphosphate to goethite. Journal of Colloid and Interface Science 367, 436–
635   442. https://doi.org/10.1016/j.jcis.2011.09.066

636 Kahiluoto, H., Kuisma, M., Ketoja, E., Salo, T., Heikkinen, J., 2015. Phosphorus in Manure
637 and Sewage Sludge More Recyclable than in Soluble Inorganic Fertilizer. Environ. Sci.
638 Technol. 49, 2115–2122. https://doi.org/10.1021/es503387y

639 Khare, N., Hesterberg, D., Beauchemin, S., Wang, S.-L., 2004. XANES Determination of
640 Adsorbed Phosphate Distribution between Ferrihydrite and Boehmite in Mixtures. Soil
641 Sci. Soc. Am. J. 68, 460–469. https://doi.org/10.2136/sssaj2004.4600

642 Kubicki, J.D., Paul, K.W., Kabalan, L., Zhu, Q., Mrozik, M.K., Aryanpour, M., Pierre-Louis,
643 A.-M., Strongin, D.R., 2012. ATR–FTIR and Density Functional Theory Study of the
644 Structures, Energetics, and Vibrational Spectra of Phosphate Adsorbed onto Goethite.
645 Langmuir 28, 14573–14587. https://doi.org/10.1021/la303111a

646 Lagos, L.M., Acuña, J.J., Maruyama, F., Ogram, A., de la Luz Mora, M., Jorquera, M.A., 2016.
647 Effect of phosphorus addition on total and alkaline phosphomonoesterase-harboring
648 bacterial populations in ryegrass rhizosphere microsites. Biol Fertil Soils 52, 1007–
649 1019. https://doi.org/10.1007/s00374-016-1137-1

650 Langmuir, I., 1918. The adsorption of gases on plane surfaces of glass, mica and platinum. J.
651 Am. Chem. Soc. 40, 1361–1403. https://doi.org/10.1021/ja02242a004

652 Leytem, A.B., Mikkelsen, R.L., Gilliam, J.W., 2002. Sorption of organic phosphorus
653 compounds in atlantic coastal plain soils: Soil Science 167, 652–658.
654 https://doi.org/10.1097/00010694-200210000-00003

655 Lü, C., Yan, D., He, J., Zhou, B., Li, L., Zheng, Q., 2017. Environmental geochemistry
656 significance of organic phosphorus: An insight from its adsorption on iron oxides.
657 Applied Geochemistry 84, 52–60. https://doi.org/10.1016/j.apgeochem.2017.05.026

658 Manning, B.A., Goldberg, S., 1996. Modeling arsenate competitive adsorption on kaolinite,
659 montmorillonite and illite. Clays and Clay Minerals 44, 609–623.
660 https://doi.org/10.1346/CCMN.1996.0440504

661 Manning, Bruce A., Goldberg, S., 1996. Modeling Competitive Adsorption of Arsenate with
662 Phosphate and Molybdate on Oxide Minerals. Soil Science Society of America Journal
663 60, 121–131. https://doi.org/10.2136/sssaj1996.03615995006000010020x

664 McKercher, R.B., Anderson, G., 1968. Characterization of the inositol penta-and
665 hexaphosphate fractions of a number of Canadian and Scottish soils. Journal of Soil
666 Science 19, 302–310.

667 Monbet, P., McKelvie, I.D., Worsfold, P.J., 2009. Dissolved organic phosphorus speciation in
668 the waters of the Tamar estuary (SW England). Geochimica et Cosmochimica Acta 73,
669 1027–1038. https://doi.org/10.1016/j.gca.2008.11.024

670 Nair, P.S., Logan, T.J., Sharpley, A.N., Sommers, L.E., Tabatabai, M.A., Yuan, T.L., 1984.
671 Interlaboratory Comparison of a Standardized Phosphorus Adsorption Procedure. J.
672 environ. qual. 13, 591–595. https://doi.org/10.2134/jeq1984.00472425001300040016x

673 Newman, R.H., Tate, K.R., 1980. Soil phosphorus characterisation by 31P nuclear magnetic
674 resonance. Communications in Soil Science and Plant Analysis 11, 835–842.

675 Ohno, T., Zibilske, L.M., 1991. Determination of Low Concentrations of Phosphorus in Soil
676 Extracts Using Malachite Green. Soil Science Society of America Journal 55, 892–895.
677 https://doi.org/10.2136/sssaj1991.03615995005500030046x

678 Parfitt, R.L., 1979. The availability of P from phosphate-goethite bridging complexes.
679 Desorption and uptake by ryegrass. Plant Soil 53, 55–65.
680 https://doi.org/10.1007/BF02181879

681 Peperzak, P., Caldwell, A.G., Hunziker, R.R., Black, C.A., 1959. Phosphorus fractions in
682 manures. Soil Science 87, 293–302.

683 Peters, J.P., Van Slyke, D.D., 1932. Quantitative clinical chemistry: J.P. Peters and D.D. Van
684 Slyke. Williams & Wilkins, Baltimore.

685 Pissarides, A., Stewart, J.W.B., Rennie, D.A., 1968. Influence of cation saturation on
686 phosphorus adsorption by selected clay minerals. Canadian Journal of Soil Science 48,
687 151–157.

688 Prietzel, J., Harrington, G., Häusler, W., Heister, K., Werner, F., Klysubun, W., 2016.
689 Reference spectra of important adsorbed organic and inorganic phosphate binding forms
690 for soil P speciation using synchrotron-based K -edge XANES spectroscopy. J
691 Synchrotron Rad 23, 532–544. https://doi.org/10.1107/S1600577515023085

692 Prietzel, J., Klysubun, W., 2018. Phosphorus K -edge XANES spectroscopy has probably often
693 underestimated iron oxyhydroxide-bound P in soils. J Synchrotron Rad 25, 1736–1744.
694 https://doi.org/10.1107/S1600577518013334

695 Rakovan, J., Becker, U., Hochella, M.F., 1999. Aspects of goethite surface microtopography,
696 structure, chemistry, and reactivity. American Mineralogist 84, 884–894.
697 https://doi.org/10.2138/am-1999-5-623

698 Reid, K., Schneider, K., McConkey, B., 2018. Components of phosphorus loss from
699 agricultural landscapes, and how to incorporate them into risk assessment tools.
700 Frontiers in Earth Science 6, 135.

701 Roy, E.D., Willig, E., Richards, P.D., Martinelli, L.A., Vazquez, F.F., Pegorini, L., Spera, S.A.,
702 Porder, S., 2017. Soil phosphorus sorption capacity after three decades of intensive
703 fertilization in Mato Grosso, Brazil. Agriculture, Ecosystems & Environment 249, 206–
704 214. https://doi.org/10.1016/j.agee.2017.08.004

705 Ruttenberg, K.C., Sulak, D.J., 2011. Sorption and desorption of dissolved organic phosphorus
706 onto iron (oxyhydr)oxides in seawater. Geochimica et Cosmochimica Acta 75, 4095–
707 4112. https://doi.org/10.1016/j.gca.2010.10.033

708 Ruyter-Hooley, M., Morton, D.W., Johnson, B.B., Angove, M.J., 2016. The effect of humic
709 acid on the sorption and desorption of myo-inositol hexaphosphate to gibbsite and
710 kaolinite: Humic acid affects phytic acid sorption. Eur J Soil Sci 67, 285–293.
711 https://doi.org/10.1111/ejss.12335

712 Shang, C., Huang, P.M., Stewart, J.W.B., 1990. Kinetics of adsorption of organic and inorganic
713 phosphates by short-range ordered precipitate of aluminum. Can. J. Soil. Sci. 70, 461–
714 470. https://doi.org/10.4141/cjss90-045

715 Sharpley, A.N., McDowell, R.W., Kleinman, P.J., 2001. Phosphorus loss from land to water:
716   integrating agricultural and environmental management. Plant and soil 237, 287–307.

717 Tisdale, S.L., Nelson, W.L., 1966. Soil Fertility and Fertilizers. Soil Science 101, 346.

718 Turner, B.L., Papházy, M.J., Haygarth, P.M., Mckelvie, I.D., 2002. Inositol phosphates in the
719   environment. Phil. Trans. R. Soc. Lond. B 357, 449–469.
720   https://doi.org/10.1098/rstb.2001.0837

721 Urrutia, O., Guardado, I., Erro, J., Mandado, M., García-Mina, J.M., 2013. Theoretical chemical
722   characterization of phosphate-metal–humic complexes and relationships with their
723   effects on both phosphorus soil fixation and phosphorus availability for plants. Journal
724   of the Science of Food and Agriculture 93, 293–303.

725 Vincent, A.G., Vestergren, J., Grobner, G., Persson, P., Schleucher, J., Giesler, R., 2013. Soil
726   organic phosphorus transformations in a boreal forest chronosequence. Plant & Soil
727   367, 149–162. https://doi.org/10.1007/s11104-013-1731-z

728 Xu, C.-Y., Li, J.-Y., Xu, R.-K., Hong, Z.-N., 2017. Sorption of organic phosphates and its
729   effects on aggregation of hematite nanoparticles in monovalent and bivalent solutions.
730   Environ Sci Pollut Res Int 24, 7197–7207. https://doi.org/10.1007/s11356-017-8382-1

731 Yan, Y.P., Liu, F., Li, W., Liu, F., Feng, X.H., Sparks, D.L., 2014. Sorption and desorption
732   characteristics of organic phosphates of different structures on aluminium
733   (oxyhydr)oxides: Sorption-desorption of organic P on Al oxyhydroxides. Eur J Soil Sci
734   65, 308–317. https://doi.org/10.1111/ejss.12119

735